RSC Advances

Heterogeneous catalytic ozonation of natural organic matter with goethite, cerium oxide and magnesium oxide

Journal:	*RSC Advances*
Manuscript ID	RA-ART-10-2015-021674.R1
Article Type:	Paper
Date Submitted by the Author:	15-Jan-2016
Complete List of Authors:	Wang, Qun; Southwest Jiaotong University, Faculty of Geosciences and Environmental Engineering Yang, Zhichao; Southwest Jiaotong University; State Key Laboratory of Urban Water Resource and Environment Chai, Bin; Southwest Jiaotong University Cheng, Shuang; Southwest Jiaotong University Lu, Xiaohui; Southwest Jiaotong University Bai, Xiaofeng; Southwest Jiaotong University
Subject area & keyword:	Heterogeneous < Catalysis

Heterogeneous catalytic ozonation of natural organic matter with goethite, cerium oxide and magnesium oxide

Qun Wang[†,*], Zhichao Yang[†,‡], Bin Chai[†], Shuang Cheng[†], Xiaohui Lu[†], Xiaofeng Bai[†]

[†]. *Faculty of Geosciences and Environmental Engineering, Southwest Jiaotong University, Chengdu 610031, P.R. China;*

[‡]. *State Key Laboratory of Urban Water Resource and Environment, Harbin Institute of Technology, Harbin 150090, P.R. China.*

* Corresponding author: Qun Wang, Phone: +86-28-66367584, E-mail: zcyang_swjtu@126.com;
Zhichao Yang, Phone: +8613654560552, E-mail: yzc096015@163.com;
Bin Chai, Phone: +8618582057537, E-mail:493775962@qq.com;
Shuang Cheng, Phone: +8618380175756, E-mail: 645678672@qq.com;
Xiaohui Lu, Phone: +8615202890282, E-mail: 879260488@qq.com;
Xiaofeng Bai, Phone: +8618581869943, E-mail: 1059591235@qq.com.

ABSTRACT

Synthetic goethite (FeOOH), magnesium oxide (MgO), and cerium oxide (CeO_2) were used as catalysts to enhance the ozonation of the filtered raw river water. The UV absorbance (At 254 nm), dissolved organic carbon (DOC), molecular weight distribution (MWD), and also excitation-emission matrix fluorescence (EEM) changes of the filtered water were evaluated before and after catalytic ozonation and single ozonation to compare the degradation efficiency of natural organic matter (NOM) in the filtered water among the systems. The results showed that CeO_2 catalytic ozonation performed best on UV_{254} removal. The addition of tert-butanol (TBA) in the systems had less effect on the removal of UV_{254}, indicating that UV_{254} removal was mainly resulted from the direct oxidation. The mineralization of NOM in the filtered water by FeOOH catalytic ozonation and MgO catalytic ozonation was significantly better than that of single ozonation and CeO_2 catalytic ozonation. DOC removal depended on hydroxyl radical (HO·) formation, which could also be verified by the changes of MWD. From the results of EEM, both fulvic acid and humic acid were oxidized effectively during catalytic ozonation and single ozonation while some differences among the systems emerged due to the different degradation mechanisms. Humic acid was oxidized followed by fulvic acid in single ozonation while they were oxidized simultaneously in the catalytic ozonation. Catalytic ozonation in the presence of MgO and FeOOH could oxidize humic acid and fulvic acid effectively due to the formation of HO·. CeO_2 catalytic ozonation would reduce fulvic acid, which was rich in carboxylate more effectively than humic acid mainly through complexation. In brief, catalytic ozonation would shorten the reaction time and also increase the mineralization of organic matter in the filtered water compared with single ozonation. This study has a certain reference value for practical application of catalytic ozonation in the water treatment plants.

Key words catalytic ozonation, NOM, filtered water, cerium oxide, synthetic goethite, magnesium oxide

1 Introduction

Natural organic matter (NOM) is the product of organisms' natural metabolic processes, most of which is humic substances-like matter containing lots of functional groups (e.g., amino

groups (-NH_2), carboxyl group (-COOH), and nitro group (-NO_2)) [1]. NOM cannot be removed effectively by conventional drinking water treatment process, which results in the microorganisms breeding in the water supply network. Even worse, NOM will react with the common disinfectants (i.e., chlorine and chloramine) to generate disinfection by-products (e.g., trihalomethanes (THMs), haloacetic acids (HAAs)), which represent a considerable health risk to human beings [2]. Thus, ozonation is widely investigated to replace chlorination to reduce the harmful by-product formation potential [3].

The published researches reported that ozone reacted fast with organic pollutants with NH_2, activated aromatics, and C=C, but slowly with compounds with inactivated aromatics, NO_2, COOH, and halogen groups (e.g., -Cl, -Br) [4, 5]. The ozone molecules can effectively translate organic compounds with unsaturated structure into that with saturated structure through the ring-opening or bond-breaking reactions. However, ozonation only changes the structure of organic matter to make them be decomposed more easily rather than decompose them into inorganic matter directly [4, 6]. It has also been confirmed that most of NOM cannot be degraded completely and sometimes toxic intermediates are produced [7].

Because of this limitation, heterogeneous catalytic ozonation, which combines ozone with solid-phase metal oxides, has been developed to improve the mineralization of NOM in drinking water without extra addition of chemicals and energy into the reaction system [8, 9]. Zhang et al. [5] studied single ozonation and synthetic goethite catalytic ozonation (O_3/FeOOH) of NOM fractions isolated from the natural water and indicated that FeOOH catalytic ozonation could enhance ozone consumption, UV absorbance (UV_{254}) removal, dissolved organic carbon (DOC) reduction and also increase the percentage of easy biodegradable organic carbon (BDOC) compared with single ozonation. In addition, the effective removal of nitrobenzene [10], oxalic acid [11] and para-chlorobenzoic acid (pCBA) [12] in the O_3/FeOOH system has been investigated, and all of the authors agreed that the degradation of organic compounds by O_3/FeOOH follows hydroxyl radical (HO·) pathway. Moreover, Zhang and Ma inferred that O_3 with nucleophilic and electrical characteristics could combine with hydroxyl groups on the surface of FeOOH to generate HO·, which was non-selective with strong oxidizing property [10]. Lee et al. [13] investigated the degradation of humic acid by Fe/MgO catalytic ozonation and found that humic acid with high molecular weight could be notably decomposed into organic compounds with low molecular weight. Azo dyes [14, 15], phenol [16, 17] and formaldehyde [18] were also used as target compounds to study the efficacy and mechanism of MgO catalytic ozonation (O_3/MgO). Some researchers reported the interaction between O_3 and the active sites on the surface of MgO promoted the generation of HO· [14, 17, 18]; there are also some researchers considering that the alkaline environment created by hydrolyzation of MgO promotes the O_3 decomposition and is responsible for the notable degradation of organic compounds [15, 16]. Dai et al. [19] studied the degradation of acetylsalicylic acid by catalytic ozonation with magnetic ceria nanometer particles and found that the surface reaction played a dominant role on the target compound removal. In addition, the great removal efficiencies of aniline and dyes [20], phenol [21] and also oxalic acid [20, 22] by cerium oxide catalytic ozonation (O_3/CeO_2) were reported in the published researches. Both the complexation of CeO_2 [19, 22] and the redox activity by Ce^{3+}/Ce^{4+} [20] were proposed for the removal of target compounds. And also, some researchers insisted that the addition of CeO_2 would inhibit the formation of HO· [21, 23].

However, most of the published researches focused on the removal of the special pollutants

in the model water and little information is available on the comprehensive evaluation of NOM removal in natural water by catalytic ozonation with MgO, CeO_2 and also FeOOH. Moreover, very few studies have been made to assess and compare the oxidation effectiveness of O_3/FeOOH, O_3/MgO and O_3/CeO_2 on both NOM removal and also the subsequent modifications of NOM in the filtered water. And thus, in the present work, MgO, CeO_2 and FeOOH were selected as catalysts to catalyze ozonation of NOM from the effluent of Mo Panshan water treatment plant in northeastern China. The selected catalysts are known as non-expensive, non-toxic, and biocompatible materials [11]. Moreover, they are different from each other in the mechanism of target compound degradation as stated above. To well understand the performances of catalytic ozonation on NOM degradation, four indexes containing UV_{254}, DOC, molecular weight distribution (MWD) and also excitation-emission matrix fluorescence (EEM) were investigated to fully reflect the changes of NOM in the filtered water before and after catalytic ozonation and single ozonation. UV_{254} shows the relative quantity of aromatic or conjugated double bonds organic matter in water [24]. DOC is a recognized indicator of NOM in surface water. The change of DOC before and after oxidation reflects the mineralization degree of the water [25]. The change of MWD before and after oxidation will reflect the change of NOM clearly and moreover, it is a good index to compare the degradation of the target compounds by different catalytic ozonation macroscopically [26]. EEM is a powerful and widely used technique for characterizing the composition of fluorescent organic matter normally found in both synthetic and natural aqueous environments [27]. EEM represents the composition of fluorescent dissolved organic matter (FDOM) through collecting the fluorescence information when the change of excitation and emission wavelengths of the samples occurs. EEM is a method with high sensitivity and good selectivity, which also has no destructive effect on the structure of the samples in the detection process.

This work, contributing to improving our understanding of catalytic ozonation of the filtered water has practical significance on designing high-efficiency water treatment process.

2 Materials and Methods

2.1 Materials and catalysts preparation

Water samples used in this study were collected from the effluent of Harbin Mo Panshan water treatment plant. The samples were stored at 4 °C. Before used, the samples were filtered through 0.45-μm fiber filters (Whatman) to remove the suspended particles. The characteristics of the filtered water were shown in Table 1.

Table 1 The characteristics of the filtered water

All reagents were purchased from Sigma-Aldrich and were used as received. Except for the HPLC-grade phosphoric acid, all other reagents were of analytic grade. The stock solutions were prepared using Milli-Q ultrapure water (resistivity 18.2 MΩ·cm) from a Millipore system.

Cerium nitrate/magnesium nitrate was calcined in air for two hours at 450 °C in a muffle furnace (YSD-5-12T, Shanghai Yaoshi Instrument Equipment Ltd.) to obtain CeO_2 and MgO. FeOOH was synthesized following the previous method described by Zhang et al. [10].

2.2 Experimental procedure

The experiments were conducted in a semi-continuous mode at room temperature (20 °C) maintained by a thermostat (THD-5015, Tianheng). 1 L of the filtered water was introduced into the reactor (capacity, 1 L) followed by the catalysts (at a dose of 100 $mg \cdot L^{-1}$ unless specified). The

gaseous ozone (150 mL·min^{-1}) produced by a DHX-SS-1G ozone generator (Harbin Jiujiu Electrochemical Engineering Ltd.) using pure oxygen as gas source was then bubbled into the reactor through a silica dispenser. The ozone concentration could be flexibly controlled by adjusting the electric current of the ozone generator. The catalysts were introduced to the reactor after the aqueous ozone concentration stabilized. And then the reactor was magnetically stirred. In addition, batch experiments were conducted to investigate the relationship between UV_{254} removal and O_3 decomposition and tert-butanol (TBA) was used to capture HO·. The dosage of TBA was 13.5 mM (see Text S1 for detailed calculation, Supporting Information) and the detailed procedures for batch experiments were described in Text S2 (Supporting Information). In the case of adsorption tests, the catalyst was added into the reactor followed by the filtered water. The reactor was then sealed and magnetically stirred. The samples were withdrawn at different intervals and were treated followed the procedure described in our former work before determined [28].

To better evaluate the stability of the catalysts, atrazine (ATZ) was selected as a model contaminant and the degradation efficiencies of ATZ in the filtered water were compared five times with the same load of recycled catalysts. The catalysts were reclaimed by filtration through glass fiber filters and rinsed with methanol and Milli-Q water several times. The detailed method for testing the stability and recyclability of the catalysts were described in Text S3 (Supporting Information).

2.2 Analytical methods

The ozone concentration in water was measured using the indigo method [29]. The ozone concentration in gas was determined by iodometric titration [30].

The UV-Vis spectrometer (Model 752, Shandong Gaomi Rainbow Analysis Instrument Ltd.) was used to determine the ultraviolet absorbance at 254 nm. DOC was measured on a TOC analyzer (Model 3100, Jena) with analytical variance of ± 0.01 mg·L^{-1} (n = 3).

The high-performance liquid chromatography (HPLC) (Waters) equipped with Ultrahydrogel^{TM} 250 column (7.8×300 mm, Waters) and a UV detector at 254 nm was used to determine the molecular weight distribution. Phosphate buffer solution (pH 7.0) was used as the eluent with the flow rate of 1 mL·min^{-1}. The injection volume was 100 µL.

The fluorescence was measured by fluorescence spectrophotometer (Jasco FP-6500) for the data acquisition at ambient temperature of 22 °C, and the EEM images were corrected for the Raman scatter and inner-filter effect [31, 32]. Each EEM was generated by scanning excitation wavelengths from 240 to 400 nm with 5 nm steps, and detecting the emission wavelengths between 300 and 550 nm with 2 nm steps. The scanning rate was 5000 nm·min^{-1}.

ATZ was measured by HPLC equipped with a Symmetry C18 column (4.6 mm × 150 mm × 5 µm, Waters) and a UV detector at 220 nm. The eluent (1 mL.min^{-1}) was a mixture of Milli-Q water and methanol (V: V = 40: 60) and the injection volumn was 100 µL. The metal ions released from the catalysts during reactions were detected by an inductively coupled plasma optical emission spectrometer (ICP-OES, Optima 8300, Perkin-Elmer, USA).

The specific surface area of the catalysts was determined on a Micromeritics ASAP2020 analyzer. X-ray diffraction (XRD) patterns (10- 80°) of the catalysts before and after reactions were obtained in an Empyrean X-ray diffractometer (PANalytical, Holland) with a Cu Kα radiation (λ= 0.15405 nm). The surface morphologies of the catalysts were analyzed with SU8010 scanning electron microscope (SEM, Hitachi, Japan).

3 Results and Discussion

3.1 Catalyst characterization

The textural and morphological properties of the selected catalysts (i.e., FeOOH, CeO_2, and MgO) including pH_{PZC}, specific surface area, pore size and also surface morphology were determined to get a better understanding of the catalytic efficacy and also the mechanisms. The data was presented in Table 2 and Fig. 1.

Table 2 The major characteristics of selected catalysts

Table 2 showed that the difference in specific surface area among the catalysts was small. CeO_2 had the highest surface area and the smallest average pore size, which was just the opposite of FeOOH. The pH_{PZC} values of the catalysts were in great agreement with the results reported by [10] and [23].

Fig. 1 SEM images and XRD patterns of the catalysts before reactions

Fig. 1 showed the SEM images and XRD patterns of CeO_2, MgO and also FeOOH before used. As observed in Figs. 1(a), 1(b) and 1(c), CeO_2 powders presented rough ball shape, and the sizes of the powders were not uniform (20-40 nm) because of aggregation; MgO powders had the elliptical plate structure with the size of 100-400 nm; FeOOH powders looked like long-strip seeds (width × length= (200-400 nm) × (400-600 nm)). The results from XRD indicated that both CeO_2 and MgO had high crystallinities while FeOOH had low crystallinity. The crystallite sizes of CeO_2, MgO and FeOOH estimated from XRD peaks using Scherrer equation were 8.156 nm, 14.186 nm and 33.559 nm, respectively. The lattice parameters of CeO_2, MgO and FeOOH agreed well with those for pure cerianite mineral (JCPDS NO. 43-1002), pure periclase mineral (JCPDS NO. 43-1002) and pure FeOOH mineral (JCPDS NO. 29-0713), respectively.

3.2 The changes of aromatic or conjugated double bonds organic matter in the filtered water

The removal of UV_{254} by adsorption, catalytic ozonation and single ozonation was shown in Fig. 2 with Milli-Q ultrapure water as blank control.

Fig. 2 Reduction of UV_{254} by adsorption, catalytic ozonation and ozonation

As shown in Fig. 2, the adsorption of UV_{254} on FeOOH, CeO_2 and MgO was limited. UV_{254} was reduced by only 0.92% for adsorption on CeO_2, which was the least among the catalysts. The removal of UV_{254} by adsorption followed the sequence as MgO (9.20%) > FeOOH (7.83%) > CeO_2 (0.92%). It was reported that there were two ways for metal oxides to adsorb UV_{254}: surface complexation and hydrophobic effect. Hu et al. has confirmed that MgO has strong adsorption of hydrophobic alkaline organic compounds which will contribute to the removal of UV_{254} [33].

In the case of catalytic ozonation and single ozonation, O_3/CeO_2 exhibited the highest removal efficiency of UV_{254} reaching 69.59%. The reduction of UV_{254} decreased in the trend O_3/CeO_2 (69.59%) > O_3 (66.82%) > O_3/MgO (49.84%) > O_3/FeOOH (43.11%). Generally, organic molecules absorb UV_{254} light primarily through the conjugated double bonds between carbon, oxygen and also nitrogen [34]. These compounds always contain benzenes, phenols, unsaturated ketones, and also unsaturated aldehydes in the natural water [35]. Some of them can be oxidized by ozone easily, while the others are ozone-resistant and are always degraded by HO· [36]. And thus, UV_{254} was reduced by oxidation via both O_3 and HO·. Meanwhile, the specific contribution

from each species, which depends on the composition of UV_{254}, could not be quantified [37]. However, taking the catalytic properties of the catalysts as summarized in Introduction into consideration, the yield of HO· in the reactions seems to be in the order O_3/FeOOH ≈ O_3/MgO > O_3 > O_3/CeO_2 and thus, the direct oxidation by O_3 seems to play a dominant role on the removal of UV_{254} in the present condition. Batch experiments were conducted to verify the speculation.

Fig. 3 Effect of TBA on (a) O_3 decomposition and (b) UV_{254} degradation during catalytic ozonation and ozonation

The effect of TBA on the catalytic ozonation and single ozonation was investigated and the results were presented in Fig. 3. As seen from Fig. 3(a), O_3 was consumed quickly in O_3/FeOOH and O_3/MgO without TBA. The ratios of the concentration of HO· and O_3 (R_{ct} values) followed the order O_3/MgO ≈ O_3/FeOOH > O_3 > O_3/CeO_2 (Text S4, Fig. S1 and Table S1 for detailed calculation and results, Supporting Information), which was in consistent with the above speculation. The presence of TBA notably reduced the rates of O_3 decomposition in the reactions except O_3/CeO_2. Fig. 3(b) showed that the effect of TBA on the removal of UV_{254} was very limited (≤ 5 %), which agreed well with the published results [38, 39]. The UV_{254} degradation was reduced in single ozonation and the O_3/CeO_2 system after adding TBA, which might be resulted from the capture of HO· by TBA in solution. The result indicated that HO· also had a positive effect on the UV_{254} degradation. However, in the O_3/MgO and O_3/FeOOH system, TBA promoted the UV_{254} removal slightly, which might be caused by the increased residual O_3 concentration in solution (Fig. 3(a)). The direct oxidation of the components, which were responsible for the absorption of UV_{254} light, was promoted due to the increase of residual O_3 concentration. Moreover, Rivas et al previously demonstrated that the addition of TBA promoted the removal of pyruvic acid in perovskite catalytic ozonation through increasing the concentration of O_3 participating in the surface reactions [40]. Since the organic compounds could adsorb on the surfaces of MgO and FeOOH (Fig. 2), the promoted UV_{254} degradation might also be resulted from the enhanced surface reactions.

In general, the ozone reacts fast with organic compounds represented by UV_{254} ($k_{ozone} > 10^5$ $M^{-1}\cdot s^{-1}$), so does HO· ($k_{HO\cdot} > 10^8$ $M^{-1}\cdot s^{-1}$) [41]. However, the highest R_{ct} value in the reactions was much lower than 1.7×10^{-7} (Table S1, Supporting Information), which was in consistent with the results reported by Elovitz and von Gunten [42]. The results indicated a better effect of direct ozonation on the degradation of UV_{254} compared with HO· oxidation. Moreover, hydroxyl radical's ability to oxidize various organic compounds also made the probability of oxidizing that with aromatic rings and conjugated double bonds lower [36]. In conculsion, the above results demonstrated that the removal of UV_{254} of the filtered water in the present condition was mainly resulted from direct ozonation in solution although both adsorption and HO· oxidation also had a positive effect.

3.3 The changes of DOC in the filtered water

Generally, O_3 only breaks the large organic molecules into smaller ones, which could be decomposed more easily. Thus, the mineralization of DOC was always thought to be the effect of HO· mainly.

Fig. 4 Reduction of the DOC by catalytic ozonation and ozonation

As can be seen from Fig. 4, the adsorption of DOC on FeOOH, CeO_2 and MgO was limited. The most significant reduction of DOC by adsorption was obtained by CeO_2 (12.69%). The main reason was that Ce(IV) on the surface of CeO_2 is a kind of strong Lewis acid (LA) with strong complexation for some carboxyl and carbonyl groups [28]. The reduction of DOC by adsorption on the catalysts was in the sequence of CeO_2 (12.69%) > MgO (9.33%) > FeOOH (1.87%). From the aspects of catalytic ozonation and ozonation, though the removal of UV_{254} by the O_3/FeOOH process was relatively low, it exhibited a strong mineralization ability of the filtered water. The degradation of DOC by O_3/FeOOH was 27.24%, much better than that by single ozonation. The degradation of DOC by the reactions was in the sequence of: O_3/FeOOH (27.24%) > O_3/MgO (18.66%) > O_3 (10.7%) > O_3/CeO_2 (2.24%).

It was supposed that the removal efficiency and adsorption capacity was inversely related. Combining with previous studies, Chandrakanth and Amy [43] investigated the effect of ozone on the colloidal stability and aggregation of particles coated with NOM and found that ozone reacted readily with the aqueous DOC compared to the adsorbed DOC. Huber et al. [44] also demonstrated that micro-pollutants adsorbed to sludge particles would not be oxidized efficiently through the estimation of O_3 mass transfer through the boundary layers on the basis of film theory. Thus, it was deduced that the lower degradation efficiency of DOC in the O_3/MgO system than that in the O_3/FeOOH system was due to the more adsorption amount of NOM, which resulted in the above results. Moreover, the adsorption of DOC on the catalysts would reduce the specific surface area and active sites, which also had an inhibitory effect on hydroxyl groups contacting with O_3 in the O_3/FeOOH system and hydrolyzation of MgO in the O_3/MgO system to generate HO·.

From Fig. 4, the degradation of DOC by the O_3/CeO_2 system was lower than that by adsorption on CeO_2. It was likely due to that complexation was the main mechanism of CeO_2 to remove organic matter as described by Zhang et al. [22]. The large molecules were broken into smaller ones with reduced aromaticity and enhanced hydrophilism, which would decrease the adsorption on the catalysts. Thus, the adsorption position of organic matter on the surface of CeO_2 would be preempted with the existence of O_3, which weakened the complexing ability of CeO_2. Moreover, the inhibition of HO· formation caused by CeO_2 also might contribute to the lower removal efficiency of DOC in the O_3/CeO_2 process.

The above research on UV_{254} and DOC was similar to that reported by Zhang et al. [5], which proposed that the adsorption, HO· formation and the diversity in hydrophobicity of the adsorbed fractions on the catalysts led to the obtained results.

3.4 The changes of molecular weight of natural organic matter in filtered water

In order to study the changes of molecular weight in catalytic ozonation and ozonation, HPLC-SEC was used to determinate the MWD at 254 nm. According to the principle of HPLC-SEC, the large organic molecules will appear earlier than the smaller ones. The figure below showed the MWD of NOM fractions before and after catalytic ozonation and ozonation.

Fig. 5 Molecular weight distribution of individual NOM fractions after ozonation and catalytic ozonation at 254nm

It can be seen from Fig. 5 that single ozonation had the weakest ability to reduce NOM of the filtered water. Compared with the untreated filtered water, the water after single ozonation had more micromolecules, which directly confirmed the above phenomenon in the degradation

of DOC.

The O_3/FeOOH process could notably reduce the concentration of macromolecules of the filtered water while the O_3/MgO process could reduce the concentration of micromolecules more effectively, which might be contributed to the adsorption of ozonated NOM [45]. The result was in accordance with the former results in UV_{254} and DOC. CeO_2 catalytic ozonation had a better effect on the removal of small fractions of NOM compared with single ozonation, which might result from the strong complexation of CeO_2 with low molecular weight organic matter in the filtered water such as carboxylic acids [46].

3.5 The changes in the structure of functional groups that EEM expressed in the filtered water

Usually NOM is contained of different fluorophores, which represent a lot of information about functional groups, structures and so on [47]. The fluorophores, such as humic-like, fulvic-like and protein-like, can be determined by characteristic peaks of EEM.

From EEM spectra of the filtered water, it could be seen that there were two EEM peaks at Ex/Em of (240 ~ 260 nm)/(420 ~ 450 nm) and Ex/Em of (300 ~ 340 nm)/(410 ~ 440 nm). According to the previous studies [48, 49], Ex/Em of (240 ~ 260 nm)/ (420 ~ 450 nm) belonged to the Type A fluorescent chromophore (Ex/Em = 260/450) (Peak A), which represented some certain structure of fulvic acid with low molecular weight in water and Ex/Em of (300 ~ 340 nm)/(410 ~ 440 nm) belonged to the Type C fluorescent chromophore (Ex/Em = 330/450 nm) (Peak C), which could represent the structure of humic acid in water [27, 50, 51].

Fig.6 EEM spectra of the NOM fractions (a) before reactions, (b-d) after 20 min adsorption by CeO_2, FeOOH and MgO, (e, g, I, k) after 10 min ozonation and catalytic ozonation, and (f, h, j, l) after 20 min ozonation and catalytic ozonation.

Table 3 The EEM peak intensities of fluorophores and the corresponding reduction after adsorption and reactions at 10 min and 20 min

The EEM spectra of the NOM fractions during catalytic ozonation and ozonation were shown in Fig. 6 and the EEM peak intensities of fluorophores and the corresponding reductions after adsorption and reactions were shown in Table 3. It could be seen from Fig. 6 (a) and Table 3, the intensity of Peak A was stronger than that of Peak C in the Ex/Em = (300 ~ 340 nm)/(410 ~ 440 nm) indicating that fulvic acid concentration was higher than that of humic acid. The ratio of their peak intensity (Peak A/Peak C) was 1.218. The intensity of Peak A was reduced 19.7% for adsorption on FeOOH, while it was reduced only 7.1% by CeO_2 and 5.6% by MgO, respectively. The same order was obtained in the reduction of the intensity of Peak C, which followed as FeOOH (18.1%) > CeO_2 (10.2%) > MgO (5.2%). From the results obtained, the adsorption proportion of humic-like acid and fulvic-like acid on FeOOH and MgO was almost the same.

Fig. 6 and Table 3 also showed that tryptophan-like fluorophores (Ex/Em = (260 ~ 290 nm)/ (300 ~ 350nm)), which was very little in the filtered water, appeared in the processes of catalytic ozonation and ozonation. The intensity of tryptophan-like fluorophores increased within 10 min which indicated that the reactions transformed more organic matter to tryptophan-like substance (Table 3). The maximum fluorescence intensity (712.288 cps) was obtained by single ozonation. As described by Świetlik and Sikorska [52], the appearance of the tryptophan-like fluorophores could be attributed to the breakdown of macromolecular proteinaceous materials by O_3, which exposed micromolecular amino groups. After then, the intensity of tryptophan-like fluorophores

continued to ascend sharply in the O_3/CeO_2 system, while, on the contrary, it was reduced sharply in single ozonation while it almost had no change in the O_3/MgO and $O_3/FeOOH$ process.

As can be seen from Figs. 6(a), 6(f), 6(h), 6(j), 6(l) and Table 3, at the end of the reaction time, the intensity of Peak A was reduced by 46.5% after single ozonation, which was the least of the reactions. It followed as: O_3/MgO (82.6%) > $O_3/FeOOH$ (74.8%) > O_3/CeO_2 (57.7%) > O_3 (46.5%). The degradation of fulvic-like acid by catalytic ozonation and single ozonation shifted the Type A fluorescent chromophore towards shorter wavelengths, which resulted in the blue-shift of fluorescence wavelength. The reduction of the intensity of Peak C followed as: O_3/MgO (84.4%) > $O_3/FeOOH$ (79.9%) > O_3 (57.3%) > O_3/CeO_2 (54.1%). It was reported that the blue-shift was mainly associated with the subsequent changes of structure and functional groups: the degradation of NOM with aromaticity into smaller molecules, the reduction of aromatic rings or conjugated bonds, or the reduction of the functional groups, like carbonyl, hydroxyl and amino groups [53]. The removal of humic acid and fulvic acid might be related with the adsorption of organic matter on the catalysts and HO· formation in single ozonation, O_3/MgO and $O_3/FeOOH$, while it might be owing to the degradation of the carboxylate in the O_3/CeO_2 process as mentioned previously.

It can also be known from Fig. 6 and Table 3, humic acid were oxidized followed by fulvic acid in single ozonation. At first, a blue-shift of Peak C appeared, which showed that the humic substances in water were oxidized into small organic molecules by single ozonation within 10 min, and then fulvic acid was further oxidized within 10-20 min. Nevertheless, they were oxidized almost simultaneously in the catalytic reactions. Moreover, the reduction of the intensity of Peak A seemed to be similar with that of Peak C at the end of reaction time.

Moreover, some comparative analysis can be done from Table 3. The O_3/MgO process was the most effective process in oxidizing both humic acid and fulvic acid. The result was opposite to the oxidation of DOC in Section 3.3. It could be contributed to the adsorption of NOM on the catalysts as stated above. In the O_3/CeO_2 system, the removal efficiency of the intensity of Peak C at the end of the reaction time was slightly higher than that at 10 min, which meant that the oxidation of Peak C had basically completed within 10 min. In the $O_3/FeOOH$ system, the oxidation of the fluorophores completed within 10 min, which was shorter than O_3/MgO and single ozonation.

From the previous researches on the characterization of humic acid and fulvic acid in China [1, 54, 55], both of humic acid and fulvic acid have a lot of functional groups, such as aliphatic groups, carbohydrate groups, aromatic groups, carboxylate and carbonyl groups etc. However, some differences could also be obtained. Humic acid always contains more aromatic groups and less carboxylate than fulvic acid. Also, carbohydrate carbons and aliphatic groups are also more abundant in fulvic acid than that in humic acid. Combining with Fig. 6 and the results obtained in Section 3.2- 3.4, it could be deduced that the degradation of NOM in the filtered water resulted from HO· oxidation, direction ozonation and also adsorption by catalysts. Single ozonation could effectively reduce the organic matter with aromatic rings or conjugated bonds, which was abundant in humic acid as shown in Fig. 2 and Fig. 6. Compared with catalytic ozonation, single ozonation was more preponderant in terms of oxidation of macromolecular humic acid, which was verified in Fig. 5. Both MgO catalytic ozonation and FeOOH catalytic ozonation could accelerate O_3 decomposition to generate HO· to promote the degradation of most of the functional groups in the filtered water. The adsorption of original organic matter and ozonated matter on the surface of FeOOH and MgO would decrease their removal efficiency seriously. The

O_3/CeO_2 process could reduce carboxylate which was more abundant in fulvic acid represented by Peak A effectively. Moreover, O_3 could directly oxidize aromatic or conjugated double bonds resulting in the reduction of Peak C. To sum up, catalytic ozonation with FeOOH and MgO would shorten the reaction time and also increase the degradation efficiency of the filtered water. CeO_2 catalytic ozonation would also accelerate the degradation of some specific functional groups compared with single ozonation; however, it performed worse than the other catalytic ozonation due to the degradation mechanism not relying on HO·.

3.6 Catalytic stability of the catalysts

The capability of the catalysts to be recovered and reused was assessed by performing the degradation reactions of ATZ in the filtered water repeatedly. The leaching of the metal ions was evaluated and the characterization of the catalysts after reactions was also carried out. The results were shown in Figs. 7, 8 and S2 (Supporting Information).

Fig. 7 The stability studies of the catalysts including evolution of the dimensionless concentration of ATZ in (a) the O_3/FeOOH system, (b) the O_3/CeO_2 system, (c) the O_3/MgO system in 5 runs, and (d) the leaching metal ions in the catalytic ozonation.

As shown in Fig. 7, the degradation rate of ATZ in the O_3/CeO_2 system was almost not reduced after being reused for five times. Slight reduction on the catalytic efficiency of FeOOH and MgO could be observed as the reuse times of the catalysts increased. ATZ degradation was reduced by ca. 4.46% and ca. 3.70% in the O_3/MgO system and the O_3/FeOOH system after five trials, respectively. The concentration of the released ferric ions, cerium ions and magnesium ions in solution were detected to be 5.5 $\mu g.L^{-1}$, 11.3 $\mu g.L^{-1}$ and 530 $\mu g.L^{-1}$, respectively (Fig. 7(d)). The leaching of magnesium ions might be caused by hydrolyzation of MgO, which agreed well with the reported mechanism [15, 16]. However, in such a low concentration, the leased magnesium ions had less effect on the safety of drinking water.

Fig. 8 SEM images of the catalysts after reactions

The catalysts after reactions were also characterized by SEM and XRD. The results were depicted in Fig. 8 and Fig. S2 (Supporting Information). As seen in Fig. 8, the SEM images showed that the surface morphologies of the catalysts were not changed. Since the catalytic activities of the catalysts were derived from the surfaces [10, 14], the unchanged surfaces also suggested that the catalytic activities could still be retained after being used from another angle. Moreover, XRD patterns of the catalysts after reactions were almost identical to those before reactions (Fig. S2, Supporting Information), indicating that the compositions of the catalysts were not changed in the catalytic reactions. The above results showed that all of the catalysts were catalytic stable and were easy to be recovered and reused in the drinking water treatments.

Conclusions

(i) Single ozonation would notably degrade NOM with strong aromaticity into smaller molecules mainly due to the selective oxidation by O_3.

(ii) Catalytic ozonation with FeOOH and MgO could effectively reduce DOC, humic-like acid and fulvic-like acid mainly through hydroxyl radical pathway. The adsorption of original NOM and ozonated NOM on the surface of the catalysts could decrease their degradation ability through preempting active sites and inhibiting HO· formation.

(iii) CeO_2 catalytic ozonation could degrade fulvic acid, which was rich in carboxyl acids more effectively than humic acid, which verified that complexation by CeO_2 mainly contributed to the degradation of NOM in the filtered water, not relying on HO· formation.

(iv) The oxidation of humic acid and fulvic acid was not synchronous in single ozonation as shown that humic acid was oxidized followed by fulvic acid while they were oxidized simultaneously in the catalytic ozonation.

(v) Catalytic ozonation would shorten the reaction time and also increase the degradation efficiency of the filtered water compared with single ozonation.

(vi) All of the catalysts were catalytic stable and could be recovered and reused.

Acknowledgements

This research was supported by Major Science and Technology Program for Water Pollution Control and Treatment (2009ZX07424-005-02) and The National Natural Science Foundation of China (51378141). We also thank Dr. Tao Zhang, Dr. Yi Yang, Dr. Da Wang, Dr. Congwei Luo and Dr. Xiaohang Yang for their help on the experiments.

References

[1] Z.Y. Tao, J. Zhang and J.J. Zhai, Characterization and differentiation of humic acids and fulvic acids in soils from various regions of China by nuclear magnetic resonance spectroscopy, *Anal. Chim. Acta.* 395 (1999): 199-203.

[2] P.C. Singer, Humic substances as precurors for potentially harmful disinfection by-products, *Water. Sci. Technol.* 40 (1999): 25-30.

[3] A.A. Mohammad and H.M. Munoz, Comparative study of ozone and MnO_2/O_3 effects on the elimination of TOC and COD of raw water at the Valmayor station, *Desalination.* 207 (2007): 179-183.

[4] U. von Gunten, Ozonation of drinking water: part I. Oxidation kinetics and product formation, *Water. Res.* 37 (2003), 1443-1467.

[5] T. Zhang, J.F. Lu, J. Ma and Z.M. Qiang, Comparative study of ozonation and synthetic goethite-catalyzed ozonation of individual NOM fractions isolated and fractionated from a filtered river water, *Water. Res.* 42 (2008): 1563-1570.

[6] C. N. Chang, Y. S. Ma and F.F. Zing, Reducing the formation of disinfection by-products by pre-ozonation, *Chemosphere.* 46 (2002): 21.

[7] B.K. Hordern, U.R. Stanislawiak, J. Świetlik and J. Nawrocki, Catalytic ozonation of natural organic matter on alumina, *Appl. Catal. B. Environ.* 62 (2006): 345-358.

[8] M. Muruganandham and J.J. Wu, Synthesis, characterization and catalytic activity of easily recyclable zinc oxide nanobundles, *Appl. Catal. B. Environ.* 80 (2008): 32-41.

[9] B. Li, X. Xu, L. Zhu, W. Ding and Q. Mahmood, Catalytic ozonation of industrial wastewater containing chloro and nitro aromatics using modified diatomaceous porous filling, *Desalination.* 254 (2010): 90-98.

[10] T. Zhang and J. Ma, Catalytic ozonation of trace nitrobenzene in water with synthetic goethite, *J. Mol. Catal. A. Chem.* 279 (2008): 82-89.

[11] M.H. Sui, L. Sheng, K.X. Lu and F. Tian, FeOOH catalytic ozonation of oxalic acid and the effect of phosphate binding on its catalytic activity, *Appl. Cata. B. Environ.* 96 (2010): 94-100.

[12] J.S. Park, H. Choi, K.H. Ahn and J.W. Kang, Removal mechanism of natural organic matter and organic acid by ozonae in the presence of goethite, *Ozone. Sci. Eng.* 26 (2004): 141-151.

[13] J.F. Lee, B.S. Jin, S.H. Cho, S.H. Han, O.S. Joo and K.D. Jung, Catalytic ozonation of humic acids with Fe/MgO, *Korean J. Chem. Eng.* 22 (2005): 536-540.

[14] G. Moussavi and M. Mahmoudi, Degradation and biodegradability improvement of the reactive red 198 azo dye using catalytic ozonation with MgO nanocrystals, *Chem. Eng. J.* 152 (2009): 1-7.

[15] Y.M. Dong, K. He, B. Zhao, Y. Yin, L. Yin and A.M. Zhang, Catalytic ozonation of azo dye active brilliant red X-3B in water with natural mineral brucite, *Catal. Commun.* 8 (2007): 1599-1603.

[16] K. He, Y.M. Dong, Z. Li, L. Yin, A.M. Zhang and Y.C. Zheng, Catalytic ozonation of phenol in water with natural brucite and magnesia, *J. Hazard. Mater.* 159 (2008): 587-592.

[17] G. Moussavi, A. Khavanin and R. Alizadeh, The integration of ozonation catalyzed with MgO nanocrystals and the biodegradation for the removal of phenol from saline wastewater, *Appl. Cata. B. Environ*. 97 (2010): 160-167.

[18] G. Moussavi, A. Yazdanbakhsh and M. Heidarizad, The removal of formaldehyde from concentrated synthetic wastewater using O_3/MgO/H_2O_2 process integrated with the biological treatment, *J. Hazard. Mater.* 171 (2009): 907-913.

[19] Q.Z. Dai, J.Y. Wang, J. Yu, J. Chen and J.M. Chen, Catalytic ozonation for the degradation of acetylsalicylic acid in aqueous solution by magnetic CeO_2 nanometer catalyst particles, *Appl. Cata. B. Environ*. 144 (2014): 686-693.

[20] C.A. Orge, J.J.M. Órfão, M.F.R. Pereira, A.M. Duarte de Farias, R.C.R. Neto and M.A. Fraga, Ozonation of model organic compounds catalysed by nanostructured cerium oxides, *Appl. Cata. B. Environ*. 103 (2011): 190-199.

[21] M.F. Pinheiro da Silva, L.S. Soeira, K.R.P. Daghastanli, T.S. Martins, I.M. Cuccovia, R.S. Freire and P.C. Isolani, CeO_2-catalyzed ozonation of phenol: the role of cerium citrate as precursor of CeO_2. J. Therm. Anal. Calorim. 102 (2010): 907- 913.

[22] T. Zhang, W.W. Li and J.P. Croué, Catalytic ozonation of oxalate with a cerium supported palladium oxide: an efficient degradation not relying on hydroxyl radical oxidation, *Environ. Sci. Technol.* 45 (2011): 9339-9346.

[23] T. Zhang, W.P. Chen, J. Ma and Z.M. Qiang, Minimizing bromate formation with cerium dioxide during ozonation of bromide-containing water, *Water. Res.* 42 (2008): 3651-3658.

[24] H.B. Kasprayk, S.U. Raczyk and J. Swiétlik, Catalytic ozonation and methods of enhancing molecular ozone reactions in water treatment, *Appl. Catal. B. Environ.* 62 (2006): 345-358.

[25] G. Cool, A. Lebel, R. Sadiq and M.J. Rodriguez, Impact of catchment geophysical characteristics and climate on the regional variability of dissolved organic carbon (DOC) in surface water, *Sci. Total. Environ.* 490 (2014): 947-956.

[26] Q. Zhou, S.E. Cabaniss and P.A. Maurice, Considerations in the use of high-pressure size exclusion chromatography (HPSEC) for determining molecular weights of aquatic humic substances, *Water. Res.* 34 (2000): 3505-3514.

[27] A. Baker, Fluorescence properties of some farm wastes: implications for water quality monitoring, *Water. Res.* 36 (2002): 189-195.

[28] Q. Wang, Z.C. Yang, J. Ma, J.C. Wang, L. Wang and M.K. Guo, Study on the mechanism of cerium oxide catalytic ozonation for controlling the formation of bromate in drinking water, *Desalin*. *Water*. *Treat.* DOI: 10.1080/19443994.2015.1079261.

[29] H. Bader and J. Hoigné, Determination of ozone in water by the indigo method, *Water. Res.* 15 (1981): 449–456.

[30] K. Rakness, G. Gordon, B. Langlais, W. Masschelein, N. Matsumoto, Y. Richard, C.M. Robson and I. Somiya, Guideline for measurement of ozone concentration in the process gas from an ozone generator, *Ozone. Sci. Eng.* 18 (1996): 209–229.

[31] D. Gerrity, S. Gamage, J.C. Holady, D.B. Mawhinney, O. Quinones, R.A. Trenholm and S.A. Snyder, Pilot-scale evaluation of ozone and biological activated carbon for trace organic contaminant mitigation and disinfection, *Water. Res.* 45 (2011): 2155-2165.

[32] B.D. Stanford, A.N. Pisarenko, D.R. Holbrook and S.A. Snyder, Pre-ozonation effects on the reduction of reverse osmosis membrane fouling in water reuse, *Ozone. Sci. Eng.* 33 (2011): 379-388.

[33] J.C. Hu, Z. Song, L.F. Chen, H.J. Yang, J.L. Li and R. Richards, Adsorption properties of MgO (111) nanoplates for the dye pollutants from wastewater, *J. Chem. Eng. Data.* 55 (2010): 3742-3748.

[34] Y.L. Song, B.Z. Dong, N.Y. Gao and S.J. Xia, Huangpu river water treatment by microfiltration with ozone pretreatment, *Desalination.* 250(2010): 71-75.

[35] R. Gracia, S. Cortes, J. Sarasa, P. Ormad and J.L. Ovelleiro, TiO_2-catalysed ozonation of raw Ebro river water, *Water. Res.* 34 (2000), 1525-1532.

[36] R. Gracia, S. Cortes, J. Sarasa, P. Ormad and J.L. Ovelleiro, Heterogeneous catalytic ozonation with supported titanium dioxide in model and natural waters, *Ozone. Sci. Eng.* 22 (2000): 461-471.

[37] E.C. Wert, F.L.R. Ortiz and S.A. Snyder, Using ultraviolet absorbance and color to assess pharmaceutical oxidation during ozonation of wastewater, *Environ. Sci. Technol.* 43 (2009): 4858-4863.

[38] S. Cortez, P. Teixeira, R. Oliveira and M. Mota, Evaluation of Fenton and ozone-based advanced oxidation processes as mature landfill leachate pre-treatments, *J. Environ. Manage.* 92 (2011): 749-755.

[39] I.A. Balcioglu and M. Ötker, Treatment of pharmaceutical wastewater containing antibiotics by O_3 and O_3/H_2O_2 processes, *Chemosphere.* 50 (2003): 85-95.

[40] F.J. Rivas, M. Carbajo, F.J. Beltrán, B. Acedo and O. Gimeno, Perovskite catalytic ozonation of pyruvic acid in water: Operating conditions influence and kinetics. *Appl. Catal. B. Environ.* 62 (2006): 93-103.

[41] U. von Gunten, Ozonation of drinking water: part II. Disinfection and by-product formation in presence of bromide, iodide or chlorine, *Water. Res.* 37 (2003): 1469-1487.

[42] M.S. Elovitz and U. von Gunten, Hydroxyl radical/ ozone ratios during ozonation processes. I. The R_{ct} concept, *Ozone. Sci. Eng*. 21 (1999): 239-260.

[43] M.S. Chandrakanth, and G.L. Amy, Effects of ozone on the colloidal stability and aggregation of particles coated with natural organic matter, *Environ. Sci. Technol.* 30 (1996): 431-443.

[44] M.M. Huber, A. Göbel, A. Joss, N. Hermann, D. Löffler, C.S. McArdell, A. Ried, H. Siegrist, T.A. Ternes and U. von Gunten, Oxidation of pharmaceuticals during ozonation of municipal wastewater effluents: a pilot study, *Environ. Sci. Technol.* 39 (2005): 4290-4299.

[45] M.T. Orta de Velásquez, A.E.C.R. Pineda, I.M. Ramirez and I.Y. Noguez, Ozone application during coagulation of wastewater: effect on dissolved matter, *Ozone. Sci. Eng.* 32 (2010): 323-328.

[46] T. Zhang and J.P.Croué, Catalytic ozonation not relying on hydroxyl radical oxidation: a selective and competitive reaction process related to metal-carboxylate complexes, *Appl.*

Catal. B. Environ. 144 (2014): 831-839.

[47] T.K. Nissinen, I.T. Miettinen and P.T. Martikainen, Molecular size distribution of natural organic matter in raw and drinking waters, *Chemosphere.* 45 (2001): 865-873.

[48] S. Elloitt, J.R. Lead and A. Baker, Characterisation of the fluorescence from fresh water, planktonic bacteria, *Water. Res.* 40 (2006): 2075-2083.

[49] R.X. Liu, J.R. Lead and A. Baker, Fluorescence characterization of cross flow ultrafiltration derived freshwater colloidal and dissolved organic matter, *Chemosphere.* 68 (2007): 1304-1311.

[50] R.X. Hao, H.Q. Ren, J.B. Li, Z.Z. Ma and H.W. Wan, Use of three-dimensional excitation and emission matrix fluorescence spectroscopy for predicting the disinfection by-product formation potential of reclaimed water, *Water. Res.* 46 (2012): 5765-5776.

[51] S. Valencia, J.M. Marín, G. Restrepo and F.H. Frimmel, Application of excitation-emission fluorescence matrices and UV/Vis absorption to monitoring the photocatalytic degradation of commercial humic acid, *Sci. Total. Environ.* 442 (2013): 207-214.

[52] J. Świetlik and E. Sikorska, Application of fluorescence spectroscopy in the studies of natural organic matter fractions reactivity with chlorine dioxide and ozone, *Water. Res.* 38 (2004): 3791-3799.

[53] A. Baker, R. Inverarity, M. Charlton and S. Richmond, Detecting river pollution using fluorescence spectrophotometry: case studies from the ouseburn, NE England, *Environ. Pollut.* 124 (2003): 57-70.

[54] M.C. He, Y.H. Shi and C.Y. Lin, Characterization of humic acids extracted from the sediments of the various rivers and lakes in China, *Sci. Total. Environ.* 20 (2008): 1284-1299.

[55] A.M. Li, M.J. Xu, W.H. Li, X.J. Wang and J.Y. Dai, Adsorption characterizations of fulvic acid fractions onto kaolinite, *J. Environ. Sci.* 20 (2008): 528-535.

Figures

The figures are in the following order:

1.

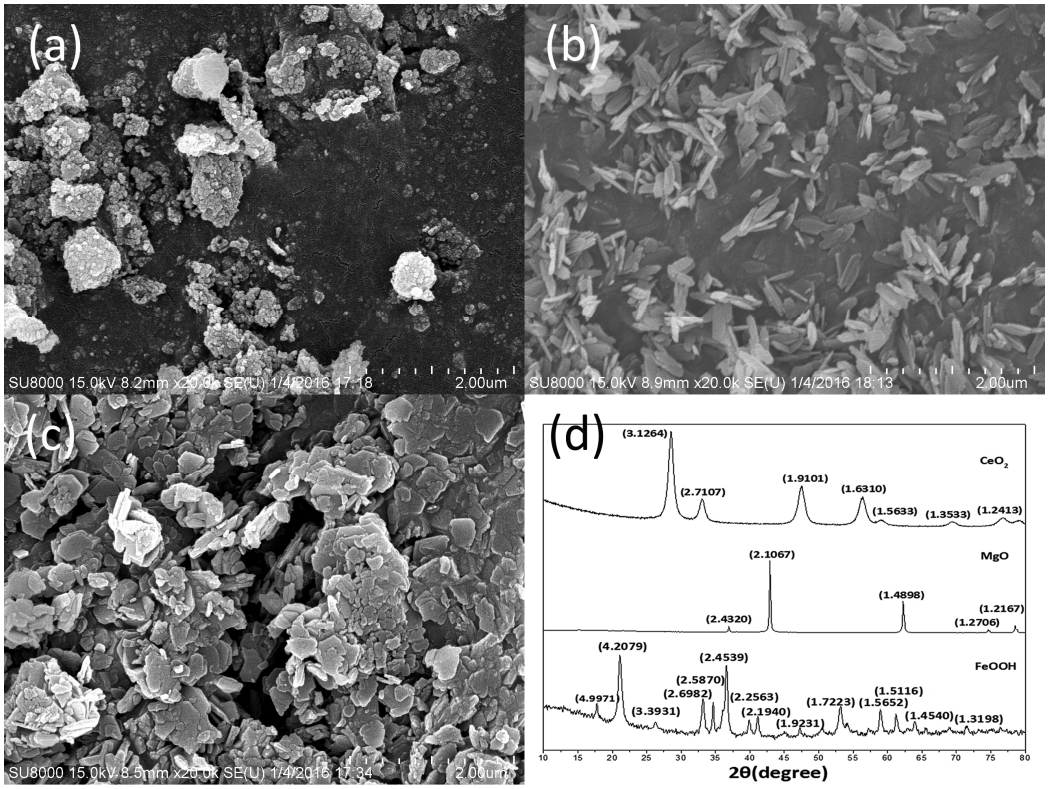

Fig. 1 SEM images of (a) CeO_2, (b) FeOOH, (c) MgO and (d) XRD patterns of the catalysts before reactions

2.

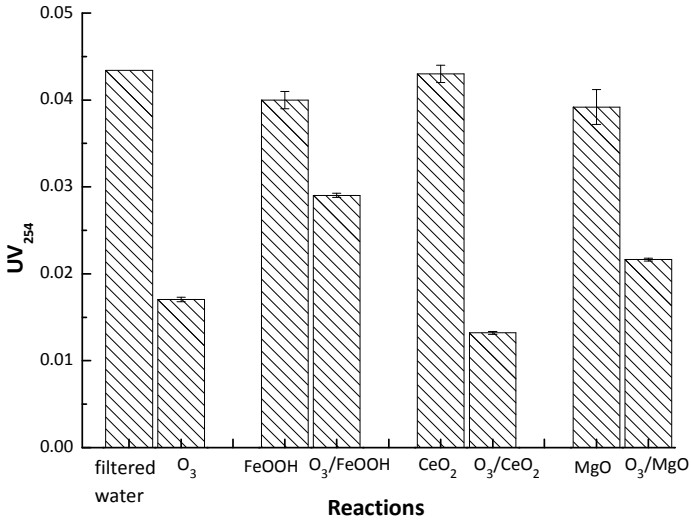

Fig. 2 Reduction of UV_{254} by adsorption and catalytic ozonation. Catalyst dose=100 mg·L^{-1}, T=20 °C, pH= 7.53, ozone gas flow rate of 150 mL·min^{-1}, ozone gas concentration of 0.15 mg·min^{-1}, reaction time = 20 min

3.

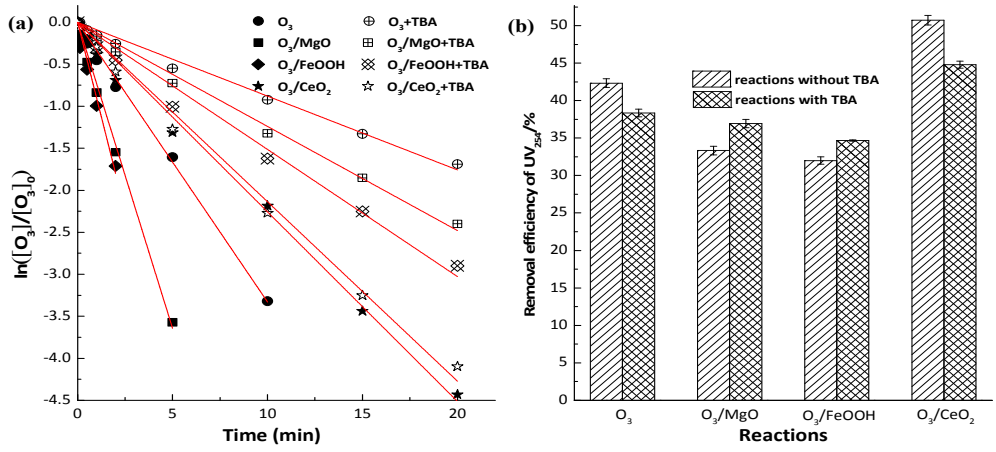

Fig. 3 Effect of TBA on (a) O_3 decomposition and (b) UV_{254} degradation during catalytic ozonation and ozonation. Catalyst dose= 100 mg·L^{-1}, T= 20 °C, pH= 7.53, $[O_3]_0$= 1.17 ± 0.03 mg·L^{-1}, $[TBA]_0$= 13.5 mM, reaction time = 20 min

4.

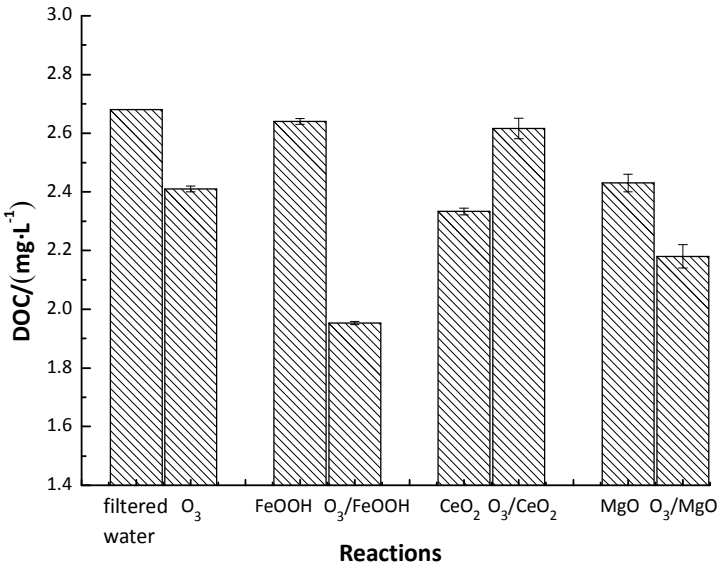

Fig. 4 Reduction of DOC by catalytic ozonation and ozonation. Catalyst dose =100 mg·L^{-1}, T=20 °C, pH= 7.53, ozone gas flow rate of 150 mL·min^{-1}, ozone gas concentration of 0.15 mg·min^{-1}, reaction time = 20 min

5.

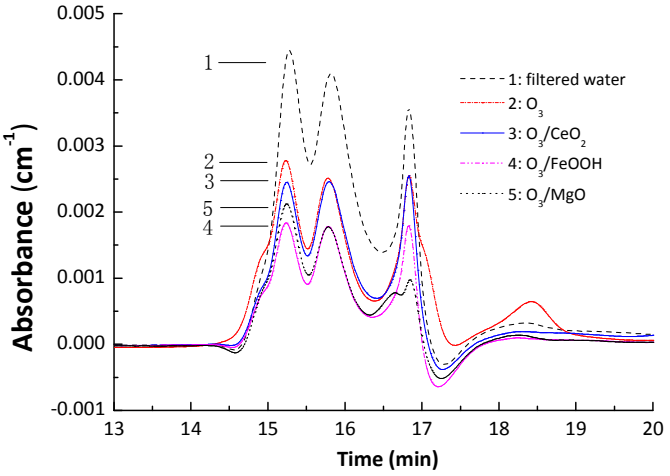

Fig. 5 Molecular weight distribution of individual NOM fractions after ozonation and catalytic ozonation at 254 nm

6.

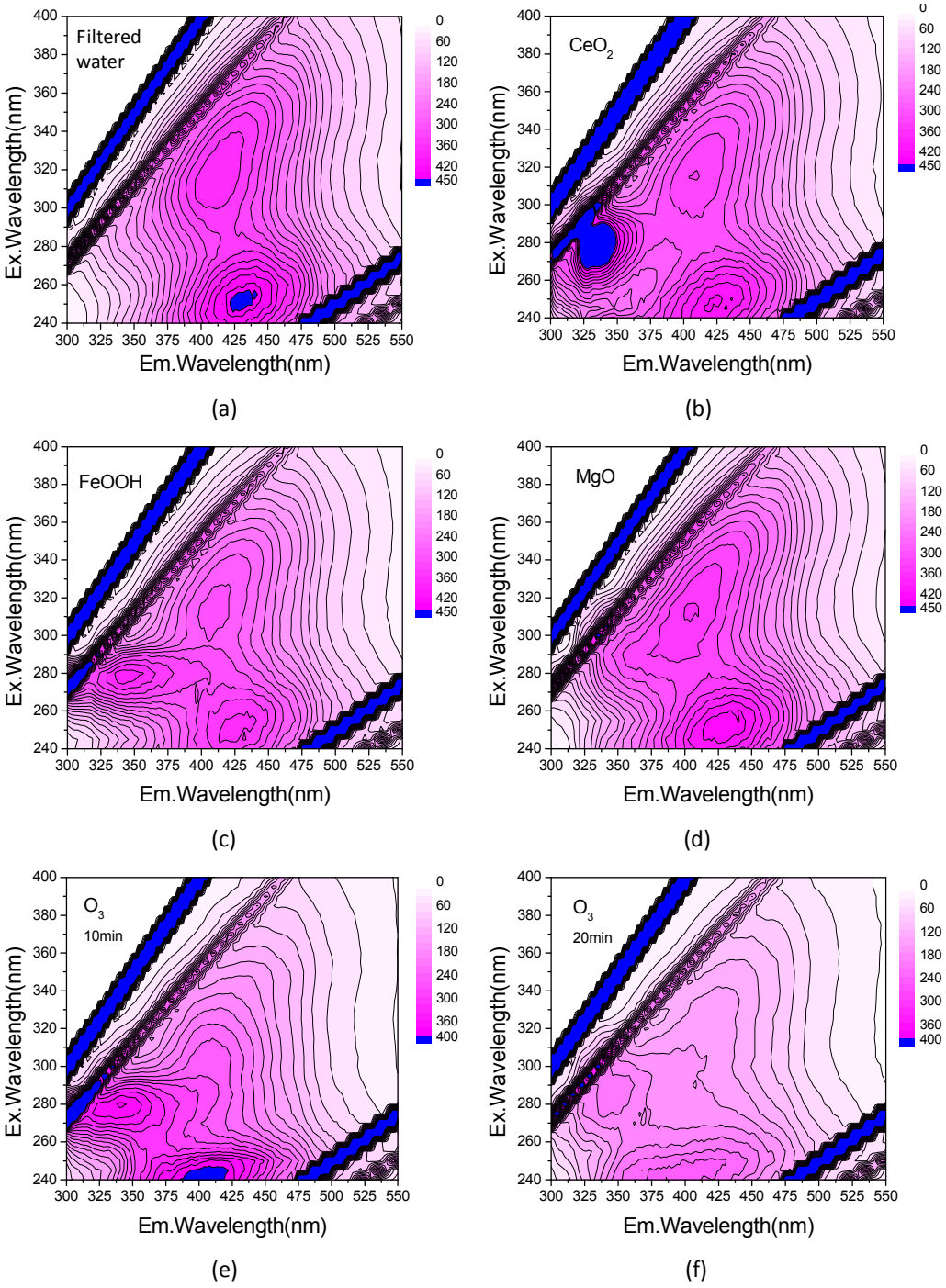
Filtered water
Ex.Wavelength(nm)
Em.Wavelength(nm)
(a)
CeO2
(b)
FeOOH
(c)
MgO
(d)
O3 10min
(e)
O3 20min
(f)

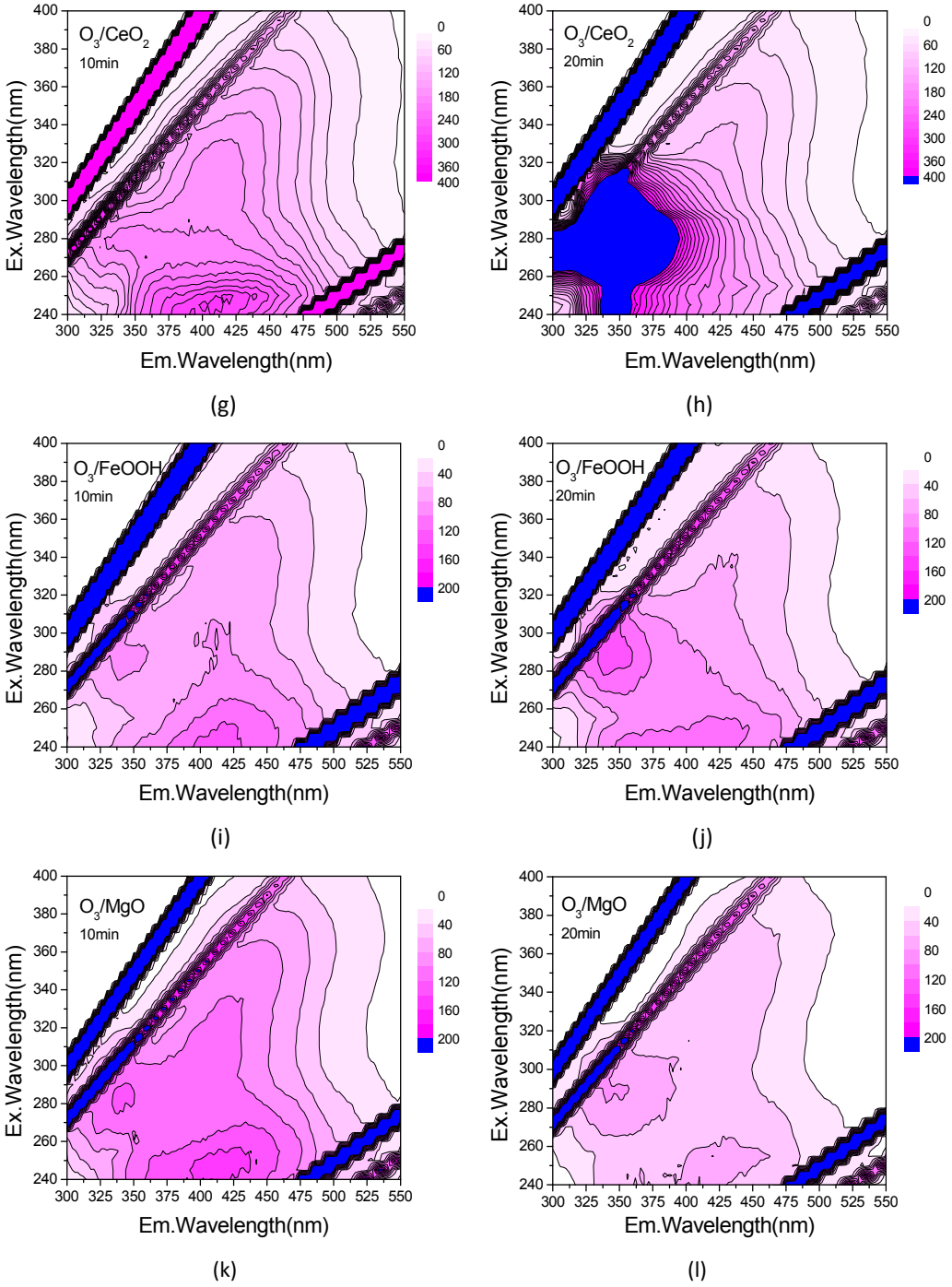

Fig. 6 EEM spectra of the NOM fractions (a) before reactions, (b-d) after 20 min adsorption by CeO_2, FeOOH and MgO, (e, g, I, k) after 10 min ozonation and catalytic ozonation, and (f, h, j, l) after 20 min ozonation and catalytic ozonation. Catalyst dose =100 $mg \cdot L^{-1}$, T=20 °C, pH= 7.53, ozone gas flow rate of 150 $mL \cdot min^{-1}$, ozone gas concentration of 0.15 $mg \cdot min^{-1}$

7.

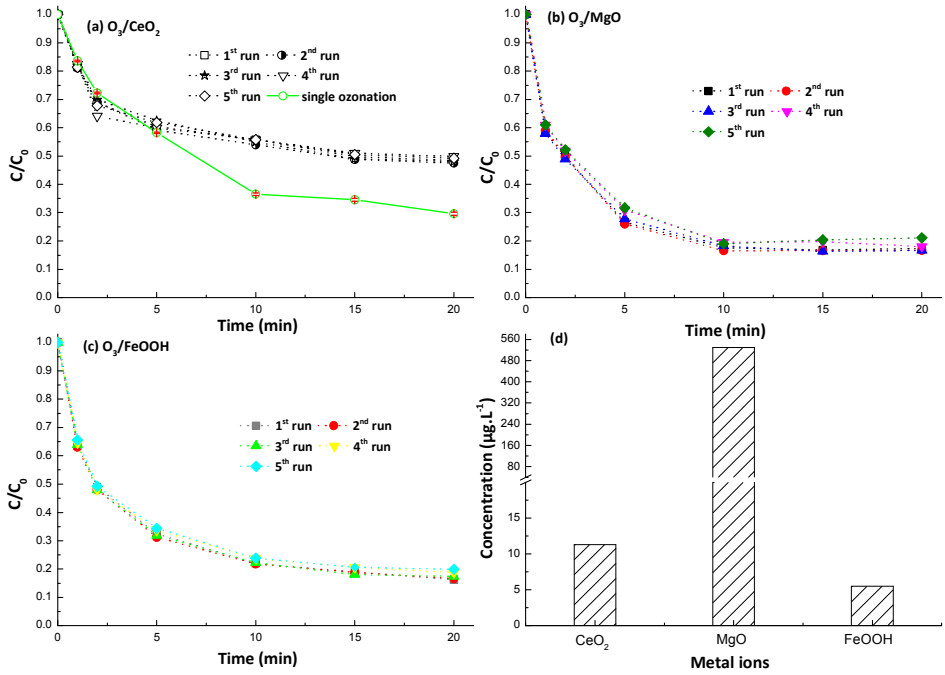

Fig.7 The stability studies of the catalysts including evolution of the dimensionless concentration of ATZ in (a) the O_3/CeO_2 system and single ozonation, (b) the O_3/MgO system, (c) the O_3/FeOOH system in 5 runs, and (d) the concentration of the leaching metal ions in the catalytic ozonation in the 1st run. Catalyst dose= 100 mg·L^{-1}, T= 20 °C, pH= 7.53, $[O_3]_0$= 1.17 ± 0.03 mg·L^{-1}, $[ATZ]_0$= 2 µM, reaction time = 20 min

8.

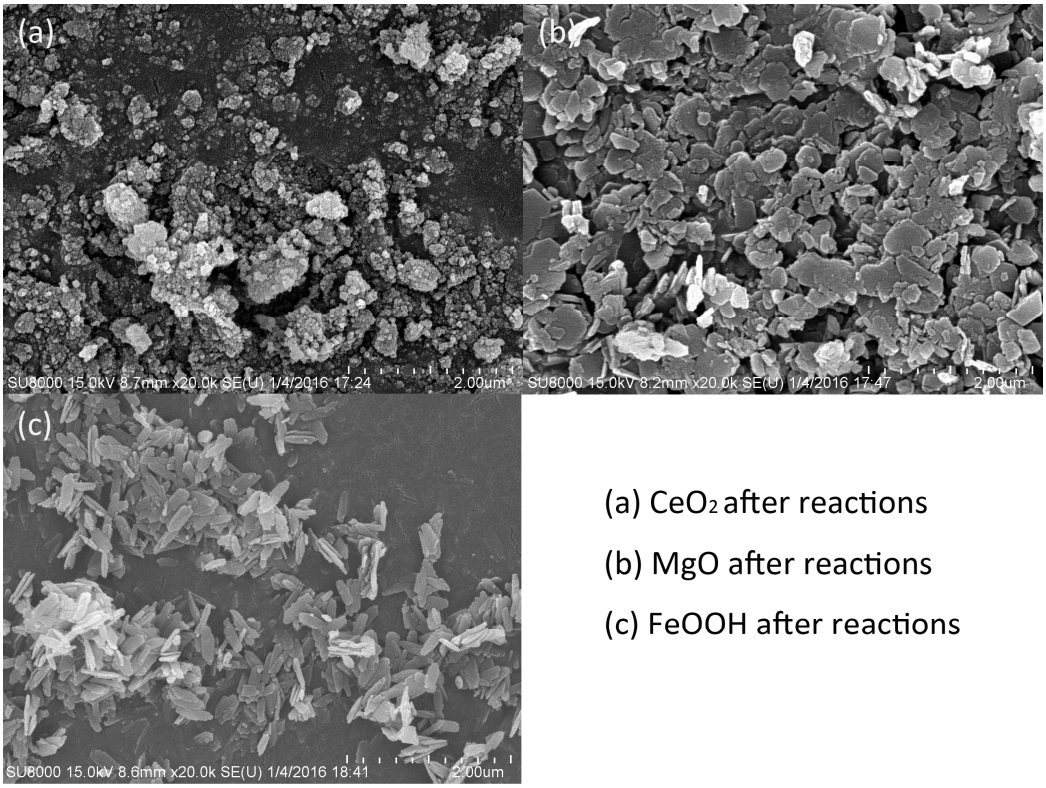

Fig.8 SEM images of the catalysts after reactions

Tables

The tables are in the following order:

1.

Table 1 The characteristics of the filtered water

DOC/(mg·L^{-1})	pH	UV_{254}/(cm^{-1})	temperature/°C
2.68	7.53	0.0434	20

2.

Table 2 The major characteristics of the selected catalysts

catalyst	pH_{PZC}	BET specific surface area/($m^2 \cdot g^{-1}$)	Average pore size/ nm
CeO_2	6.7	116 ± 2.2	12.6
FeOOH	6.8	97 ± 1.4	23.2
MgO	11.1	105 ± 1.5	16.7

3.

Table 3 The EEM peak intensities of fluorophores and the corresponding reduction after adsorption and reactions at 10min and 20 min

Indexs	Type A fluorophores		Type C fluorophores		Tryptophan-like fluorophores
	Intensity/cps	Reduced proportion/%	Intensity/cps	Reduced proportion/%	Intensity/cps
Filtered water	462.569	_	379.809	_	_
CeO_2(20min)	429.854	7.1	341.194	10.2	_
FeOOH(20min)	371.456	19.7	311.298	18.1	_
MgO(20min)	436.643	5.6	360.070	5.2	_
O_3(10min)	404.261	12.6	254.361	33.0	712.288
O_3/CeO_2(10min)	304.137	34.2	176.965	53.4	491.484
O_3/FeOOH(10min)	130.861	71.7	81.6502	78.5	407.393
O_3/MgO(10min)	151.080	67.3	109.283	71.2	444.072
O_3(20min)	247.615	46.5	162.156	57.3	482.331
O_3/CeO_2(20min)	195.596	57.7	174.275	54.1	999.999
O_3/FeOOH(20min)	116.580	74.8	76.1536	79.9	435.636
O_3/MgO(20min)	80.5261	82.6	59.4001	84.4	420.592

Note: Reduced proportion/% = (intensity reduced by adsorption)/(initial intensity of NOM)×100%

GRAPHICAL ABSTRACT for

Heterogeneous catalytic ozonation of natural organic matter with goethite, cerium oxide and magnesium oxide